fractal and fractional

Article

Complex Dynamics Analysis and Chaos Control of a Fractional-Order Three-Population Food Chain Model

Zhuang Cui [1], Yan Zhou [1,2,*] and Ruimei Li [1]

[1] College of Mathematics Science, Inner Mongolia Normal University, Hohhot 010022, China; 20224012016@mails.imnu.edu.cn (Z.C.); 20224012021@mails.imnu.edu.cn (R.L.)
[2] Center for Applied Mathematical Science, Inner Mongolia Normal University, Hohhot 010022, China
* Correspondence: 20130022@imnu.edu.cn

Abstract: The present study investigates the stability analysis and chaos control of a fractional-order three-population food chain model. Previous research has indicated that the predation relationship within a long-established predator–prey system can be influenced by factors such as the prey's fear of the predator and its carry-over effects. This study examines the state evolution of fractional-order systems and compares their dynamic behavior with integer-order systems. By utilizing the Routh–Hurwitz condition and the stability theory of fractional differential equations, this paper establishes the local stability conditions of the model through the application of the Jacobi matrix and eigenvalue method. Furthermore, the conditions for the Hopf bifurcation generation are determined. Subsequently, chaos control techniques based on the Lyapunov stability theory are employed to stabilize the unstable trajectory at the equilibrium point. The theoretical findings are validated through numerical simulations. These results enhance our understanding of the stability properties and chaos control mechanisms in fractional-order three-population food chain models.

Keywords: stability analysis; chaos control; fractional derivative; Hopf bifurcation; three-population model

Citation: Cui, Z.; Zhou, Y.; Li, R. Complex Dynamics Analysis and Chaos Control of a Fractional-Order Three-Population Food Chain Model. *Fractal Fract.* **2023**, *7*, 548. https://doi.org/10.3390/fractalfract7070548

Academic Editor: Ivanka Stamova

Received: 25 June 2023
Revised: 12 July 2023
Accepted: 14 July 2023
Published: 16 July 2023

1. Introduction

The study of population models remains a prominent area of research [1,2]. Various mathematical models have been proposed to investigate the dynamic behavior of populations, encompassing ordinary differential equation models, partial differential equation models [3], fractional differential equation models [4–7], stochastic models [8], models with time delays [9], models with state feedback control [10], network models [11], and more. In 1959, Holling et al. introduced the Holling model [12], which incorporates the functional response of predators and the growth term of prey. In 1991, Hasting and Powell [13] expanded on the Holling model and pioneered the study of chaotic dynamic behavior in three-population food chain models. Consequently, the control and harnessing of chaos have emerged as essential topics in mechanics (e.g., pendulum, plate, and friction control), communication [14], ecology, and medicine [15]. In ecology, researchers strive to utilize biological factors to control the dynamic behavior of systems. Ghosh et al. [16] investigated the Allee effect as a biological factor influencing predators. People modified and enhanced the model by incorporating biological factors, such as the Allee effect and defense, fear, migration, and delay effects. This paper primarily focuses on the impact of the fear effect on population relationships. Fear profoundly influences ecosystems, particularly certain predators that can alter the feeding behavior of multiple organisms. Notably, through sound induction, Liana Zanette reintroduced fear of predators to a group of carefree raccoons. Her study [17] revealed that when the sound of barking was broadcast, raccoons spent nearly two-thirds less time foraging in the intertidal area, resulting in an 81% increase in fish populations and a 60% increase in worms and red stone crabs. Wang et al. [18] investigated the influence of fear on prey growth in their modeling, highlighting its significant impact on the dynamic behavior of predator–prey models. Panday et al. [19] examined a food chain model incorporating fear of predation and demonstrated that appropriate fear levels could enhance the system's stability. The researchers suggested that induced fear could serve as a control strategy with important implications for preventing species extinction.

In ecology, carry-over effects (COE) refer to the influence of past learning behavior on the present behavior of a species. A carry-over effect is observed when individuals from a new colony exhibit behavior influenced by previous events. Although carry-over effects are common in animal and plant systems, they are seldom studied. Fear induction has been proposed as a form of carry-over effect. Sasmal et al. [20] developed a model considering the Allee effect caused by fear's cost of predation and its legacy effect while investigating the influence of fear on the system's dynamic behavior. Elliott et al. [21] examined fear-induced seasonal behavior. Dubey and Sasmal [22] proposed a phytoplankton–zooplankton–fish system in which zooplankton growth rates are affected by fish-induced fear and COE. They noted that the system exhibits chaotic behavior for moderate COE parameter values, while stability or periodic dynamics occur for lower and higher values. Mondal et al. [23] studied the dynamics of the Holling II type predator–prey system and the influence of carry-over effects, demonstrating that fear and its carry-over effects substantially impact the stability of the internal equilibrium point. Thus, incorporating COE into ecological models provides a deeper understanding of the factors influencing species within ecosystems.

Fractional-order models have found applications and extensions in various domains, including circuit systems [24], ecological models [25–27], rheology [28], control engineering [29], reflection diffusion [30], and chaos models [31]. Fractional derivatives offer a more realistic depiction as they consider the entire time region of a biological process, whereas integer derivatives only capture changes at specific points in time [26]. Adopting fractional derivatives in ecological models enriches the results compared to integer derivatives and allows for better fitting of realistic data through appropriate order selection. The fractional derivative provides a novel approach for accurately describing the dynamic behavior of ecosystems characterized by heritability and long memory. Researchers have investigated various fractional models to improve the accuracy of results. Ji et al. [32] examined fractional two-species systems and provided parameters for stable systems. Das [33] systematically introduced fractional differential equations and their applications. Mishra [27] studied the dynamic behavior of the fractional-order three-population food chain model. Tavazoei et al. [34] demonstrated that the limit set of trajectories in fractional-order systems might not correspond to the solution of the system, diverging from integer-order systems. Tavazoei et al. [35,36] proved the non-existence of periodic solutions in time-invariant fractional-order systems. They presented a system with non-periodic trajectories converging to periodic signals.

This study investigates a fractional-order three-population food chain model incorporating fear and carry-over effects. The primary research objectives are as follows. Firstly, the local stability of the model is analyzed using the fractional order theory. The conditions for fractional Hopf bifurcation are examined, and stability conditions for the equilibrium point under different circumstances are provided. Secondly, a hybrid control method is employed to guide the unstable trajectory toward convergence with the equilibrium point. It is demonstrated that the fractional order can induce changes in the stability of system. Finally, the numerical simulation is conducted to validate the theoretical analysis. This study extends the work previously conducted by Ramasamy et al. [1].

2. Preliminary Knowledge

Definition 1. *The Caputo fractional derivative of order $\alpha \in (n-1, n]$, $n \in N$ of $f(t)$ is defined as:*

$$ {}_a^cD_t^\alpha f(t) = I^{n-\alpha}\left(\frac{\mathrm{d}^n}{\mathrm{d}t^n} f(t)\right) = \frac{1}{\Gamma(n-\alpha)} \int_a^t f^n(\tau)(t-\tau)^{n-\alpha-1} \mathrm{d}\tau, \quad t > a. \tag{1}$$

Theorem 1 ([37]). *Let $x(t) \in R$ be a continuous and derivable function, then for any time instant $t \geq a$:*

$$\frac{1}{2}{}_a^c D_t^\alpha x^2(t) \leq x(t) {}_a^c D_t^\alpha x(t). \tag{2}$$

Theorem 2. *Consider the fractional-order system given below:*

$$D^\alpha x(t) = f(x(t)), \quad x(0) = x_0 \in \mathbb{R}^N, \quad 0 < \alpha < 1, \tag{3}$$

where $x(t) = (x_1(t), x_2(t), \cdots, x_N(t))^T \in \mathbb{R}^N$ and f: $(f_1, f_2, \cdots, f_N)^T$: $\mathbb{R}^N \to \mathbb{R}^N$. The equilibrium points of system (3) are determined by solving the equation $f(x) = 0$.

We suppose x^* is an equilibrium point of system (3) and the Jacobian matrix $J = \frac{\partial f}{\partial x} = \frac{\partial(f_1, f_2, \cdots, f_N)}{\partial(x_1, x_2, \cdots, x_N)}$. The equilibrium point x^* is locally asymptotically stable, for all eigenvalues λ_i of J, if and only if $\min\limits_{1 \leq i \leq 3} |\arg(\lambda_i)| > \frac{\alpha\pi}{2}$. This is easy to obtain, though the equilibrium x^* is unstable when the following condition holds $\min\limits_{1 \leq i \leq 3} |\arg(\lambda_i)| \leq \frac{\alpha\pi}{2}$. The above results was proved in Matignon [38].

3. Systems Description

In [1], the author constructed and considered an integer-order system, given below:

$$\begin{cases} \dfrac{\mathrm{d}U(t)}{\mathrm{d}T} = R_0 U(1 - \dfrac{U}{K}) \cdot \dfrac{1 + E_1 U}{1 + E_2 U + F_1 V} - \dfrac{C_1 A_1 U V}{B_1 + U}, \\ \dfrac{\mathrm{d}V(t)}{\mathrm{d}T} = \dfrac{A_1 U V}{B_1 + U} \cdot \dfrac{1 + E_2 V}{1 + E_2 V + F_2 W} - D_1 V - \dfrac{A_2 V W}{B_2 + V}, \\ \dfrac{\mathrm{d}W(t)}{\mathrm{d}T} = \dfrac{C_2 A_2 V W}{B_2 + V} - D_2 W, \end{cases} \tag{4}$$

where $U(T)$, $V(T)$, and $W(T)$ are the respective densities of prey, middle, and special predators at time T. To simplify the notation, the state variables $U(T)$, $V(T)$, and $W(T)$ are denoted by U, V, and W, respectively. All parameters see Table 1 of the system (4) are considered positive.

As a real model, subject to positive initial conditions, system (4) has the following initial values: $U(0) \geq 0$, $V(0) \geq 0$, and $W(0) \geq 0$.

Table 1. Parameters and their definitions.

Parameter	Biological Meaning
R_0	The intrinsic growth rate of the prey
K	Environmental carrying capacity
A_1	The maximum attack rate of the middle predator
A_2	The maximum attack rate of the special predator
B_1	The half-saturation coefficient of the prey
B_2	The half-saturation coefficient of the middle predator
C_1	Indicates the conversion efficiencies of the middle predator
C_2	Indicates the conversion efficiencies of the special predator
D_1	The death rate of the middle predator
D_2	The death rate of the special predator
F_1	The intensity of fear in the prey population
F_2	The intensity of fear in the middle predator population
E_1	The carry-over effect parameter due to the fear F_1
E_2	The carry-over effect parameter due to the fear F_2

To minimize the complexity of the system, system (4) is transformed by taking $U = K\eta_1$, $V = \frac{K}{C_1}\eta_2$, $W = \frac{C_2 K}{C_1}\eta_3$, $T = \frac{t}{R_0}$, $\alpha_1 = \frac{A_1 K}{R_0 B_1}$, $\alpha_2 = \frac{A_2 C_2 K}{R_0 B_2 C_1}$, $\beta_1 = \frac{K}{B_1}$, $\beta_2 = \frac{K}{C_1 B_2}$,

$\delta_1 = \frac{D_1}{R_0}$, $\delta_2 = \frac{D_3}{R_0}$, $f_1 = \frac{F_1 K}{C_1}$, $f_2 = \frac{F_2 C_2 K}{C_1}$, $e_1 = E_1 K$, and $e_2 = \frac{E_2 K}{C_1}$. As a result, the following system was obtained:

$$\begin{cases} \frac{\mathrm{d}\eta_1}{\mathrm{d}t} = \eta_1 \left((1-\eta_1) \cdot \frac{1+e_1\eta_1}{1+e_1\eta_1+f_1\eta_2} - \frac{\alpha_1\eta_2}{1+\beta_1\eta_1} \right), \\ \frac{\mathrm{d}\eta_2}{\mathrm{d}t} = \eta_2 \left(\frac{\alpha_1\eta_1}{1+\beta_1\eta_1} \cdot \frac{1+e_2\eta_2}{1+e_2\eta_2+f_2\eta_3} - \delta_1 - \frac{\alpha_2\eta_3}{1+\beta_2\eta_2} \right), \\ \frac{\mathrm{d}\eta_3}{\mathrm{d}t} = \eta_3 \left(\frac{\alpha_2\eta_2}{1+\beta_2\eta_2} - \delta_2 \right). \end{cases} \tag{5}$$

The following parameters were considered by [1]:

$$\alpha_1 = 5, \alpha_2 = 0.1, \beta_1 = 3, \beta_2 = 2, \delta_1 = 0.4, \delta_2 = 0.01, f_1 = 0, f_2 = 1, e_1 = 0, e_2 = 2.85, \tag{6}$$

For the initial value $(\eta_1, \eta_2, \eta_3) = (0.7, 0.1, 6)$, the system (5) has a positive Lyapunov exponent, as follows: $LE_1 = 0.0019705, LE_2 = -0.0026498, LE_3 = -0.40525$. The dynamic behavior of the system (5) is shown in Figure 1.

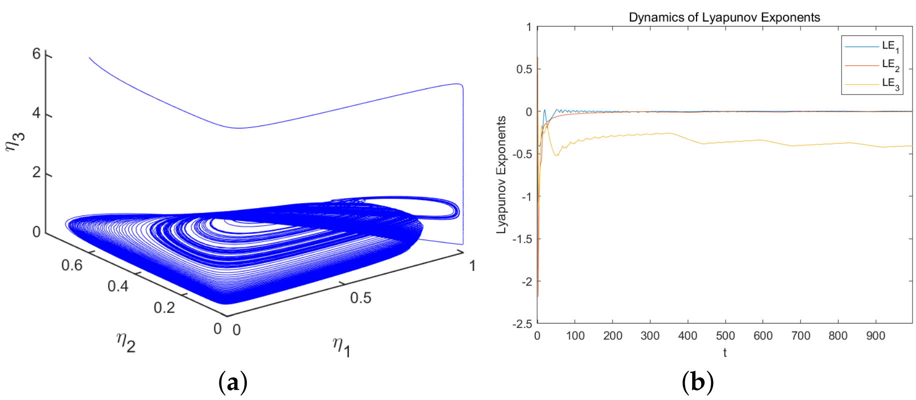

Figure 1. Phase—space diagram (**a**) and Lyapunov Exponents diagram (**b**) for system (5).

As shown in Figure 2, the parameter e_2 of the carry-over effects caused by the fear f_2 is taken as an example. It was observed that the fear-induced carry-over effects parameters changed the dynamic behavior of the system.
Case 1: If f_1, f_2, and e_1 are fixed and e_2 changes, the dynamic behavior of the system is shown in Figure 2 after selecting appropriate e_2 value.

(i) For $e_2 < 1.361$, the solution trajectories is stable, which is shown in Figure 2a.
(ii) For $e_2 \geq 1.361$, system (5) exhibits periodic oscillations, which is shown in Figure 2b.

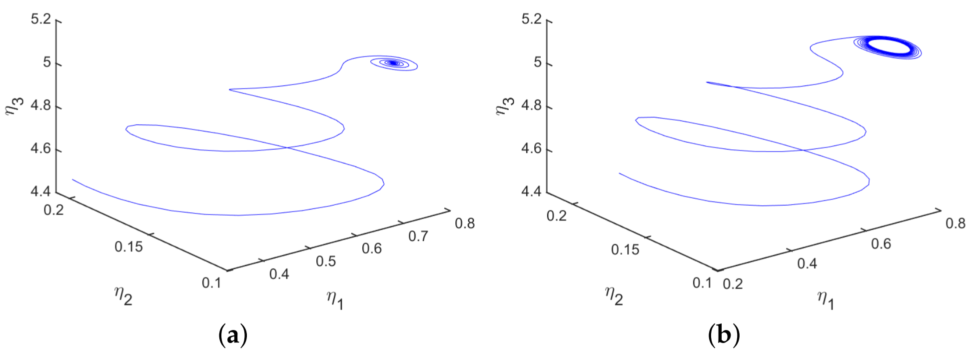

Figure 2. The phase space diagram of system (5) for different values of e_2: (**a**) LAS for $e_2 = 1$ and (**b**) periodic oscillation for $e_2 = 1.4$. The remaining parameters are assigned the values specified in Equation (6), except for $f_1 = 3.5$, $f_2 = 0.1$ and $e_1 = 1$.

The choice to utilize fractional-order differential Equations (FDE) instead of integer-order systems is motivated by their ability to mitigate errors arising from neglected parameters in applications [39]. The following system is obtained by substituting the integer-order derivative with the Caputo fractional derivative. The resulting FDE is as follows:

$$\begin{cases} \dfrac{d^{\alpha}\eta_1}{dt^{\alpha}} = \eta_1\left((1-\eta_1)\cdot\dfrac{1+e_1\eta_1}{1+e_1\eta_1+f_1\eta_2} - \dfrac{\alpha_1\eta_2}{1+\beta_1\eta_1}\right), \\ \dfrac{d^{\alpha}\eta_2}{dt^{\alpha}} = \eta_2\left(\dfrac{\alpha_1\eta_1}{1+\beta_1\eta_1}\cdot\dfrac{1+e_2\eta_2}{1+e_2\eta_2+f_2\eta_3} - \delta_1 - \dfrac{\alpha_2\eta_3}{1+\beta_2\eta_2}\right), \\ \dfrac{d^{\alpha}\eta_3}{dt^{\alpha}} = \eta_3\left(\dfrac{\alpha_2\eta_2}{1+\beta_2\eta_2} - \delta_2\right), \end{cases} \tag{7}$$

where $\alpha \in (0,1]$. In particular, when $\alpha = 1$, the system (7) simplifies to the well-known integer-order system.

4. Analysis of the Local Stability of the Equilibrium Point

4.1. Existence of Equilibrium Points

For equilibrium points, we consider the following equation:

$$\begin{cases} \eta_1\left((1-\eta_1)\cdot\dfrac{1+e_1\eta_1}{1+e_1\eta_1+f_1\eta_2} - \dfrac{\alpha_1\eta_2}{1+\beta_1\eta_1}\right) = 0, \\ \eta_2\left(\dfrac{\alpha_1\eta_1}{1+\beta_1\eta_1}\cdot\dfrac{1+e_2\eta_2}{1+e_2\eta_2+f_2\eta_3} - \delta_1 - \dfrac{\alpha_2\eta_3}{1+\beta_2\eta_2}\right) = 0, \\ \eta_3\left(\dfrac{\alpha_2\eta_2}{1+\beta_2\eta_2} - \delta_2\right) = 0. \end{cases} \tag{8}$$

The following four equilibrium points of system (7) are determined by solving the above equations: $E_0 = (0,0,0)$,$E_1 = (1,0,0)$, $E_2 = (\eta_{21}, \eta_{22}, 0)$, and $E_3 = (\eta_1^*, \eta_2^*, \eta_3^*)$, where:

$$\eta_{21} = \frac{\delta_1}{\alpha_1 - \delta_1\beta_1}, \tag{9}$$

$$\eta_{22} = \frac{-(1+e_1\eta_{21}) + \sqrt{(1+e_1\eta_{21})^2 + 4\alpha_1^{-1}f_1(1-\eta_{21})(1+e_1\eta_{21})(1+\beta_1\eta_{21})}}{2f_1}. \tag{10}$$

If $\eta_{21} < 1$ and $0 < \frac{\delta_1}{\alpha_1-\delta_1\beta_1} < 1$, it is evident that E_2 exists. When $\eta_{21} < 1$, the system (7) has the special predator-free equilibrium point.

After solving the following equation and obtaining the positive real roots, η_1^*, η_2^*, and η_3^* are obtained:

$$\begin{cases} (1-\eta_1)\cdot\dfrac{1+e_1\eta_1}{1+e_1\eta_1+f_1\eta_2} - \dfrac{\alpha_1\eta_2}{1+\beta_1\eta_1} = 0, \\ \dfrac{\alpha_1\eta_1}{1+\beta_1\eta_1}\cdot\dfrac{1+e_2\eta_2}{1+e_2\eta_2+f_2\eta_3} - \delta_1 - \dfrac{\alpha_2\eta_3}{1+\beta_2\eta_2} = 0, \\ \dfrac{\alpha_2\eta_2}{1+\beta_2\eta_2} - \delta_2 = 0. \end{cases} \tag{11}$$

Clearly, $\eta_2^* = \frac{\delta_2}{\alpha_2-\beta_2\delta_2}$ and $\alpha_2 > \beta_2\delta_2$. By making $\eta_2 = \eta_2^*$ in Equation (11), we obtain:

$$e_1\beta_1\eta_1^3 + k_1\eta_1^2 + k_2\eta_1 + k_3 = 0 \tag{12}$$

In Equation (12), $k_1 = e_1 + \beta_1 - e_1\beta_1$, $k_2 = \alpha_1 e_1\eta_2^* + 1 - e_1 - \beta_1$, and $k_3 = \alpha_1\eta_2^*(1 + f_1\eta_2^*) - 1$. If $k_i > 0$, for $i = 1,2,3$, Equation (12) cannot have positive roots. Equation (12) has at least one positive root for any one negative k_i. η_1^* is the positive root of Equation (12). Now, η_3^* is obtained by the following equation:

$$\frac{\alpha_2 f_2}{1+\beta_2\eta_2^*}\eta_3^2 + \left(\frac{\alpha_2(1+e_2\eta_2^*)}{1+\beta_2\eta_2^*} + \delta_1 f_2\right)\eta_3 - (1+e_2\eta_2^*)\left(\frac{\alpha_1\eta_1^*}{1+\beta_1\eta_1^*} - \delta_1\right) = 0. \tag{13}$$

If $\frac{\alpha_1\eta_1^*}{1+\beta_1\eta_1^*} > \delta_1$, Equation (13) gives a sufficient condition for positive roots. The coordinate of the special predator, denoted as η_3^*, corresponds to the positive root of Equation (13). Based on the analysis as mentioned earlier, it can be inferred that in practical scenarios, for the special predators to thrive, the death rate of the middle predator must remain below the critical threshold value ϕ_0, where $\phi_0 = \frac{\alpha_1\eta_1^* R_0}{1+\beta_1\eta_1^*}$. Reasonable control of the number of middle predators is conducive to promoting ecological prosperity and development. Therefore, the middle predators play an important role in the ecosystem system.

4.2. Local Stability Analysis

The Jacobian matrix of the system (7) at any point $\overline{E}(\overline{\eta_1}, \overline{\eta_2}, \overline{\eta_3})$ is given below:

$$J(\overline{E}) = \begin{bmatrix} a_{11} & a_{12} & 0 \\ a_{21} & a_{22} & a_{23} \\ 0 & a_{32} & a_{33} \end{bmatrix}, \tag{14}$$

where

$$\begin{aligned}
a_{11} &= \frac{1-2\overline{\eta_1}+2e_1\overline{\eta_1}-3e_1\overline{\eta_1}^2}{1+e_1\overline{\eta_1}+f_1\overline{\eta_2}} - \frac{e_1\overline{\eta_1}(1-\overline{\eta_1})(1+e_1\overline{\eta_1})}{(1+e_1\overline{\eta_1}+f_1\overline{\eta_2})^2} - \frac{\alpha_1\overline{\eta_2}}{(1+\beta_1\overline{\eta_1})^2}, \\
a_{12} &= -\frac{f_1\overline{\eta_1}(1-\overline{\eta_1})(1+e_1\overline{\eta_1})}{(1+e_1\overline{\eta_1}+f_1\overline{\eta_2})^2} - \frac{\alpha_1\overline{\eta_1}}{1+\beta_1\overline{\eta_1}}, a_{21} = \frac{\alpha_1(1+e_2\overline{\eta_2})\overline{\eta_2}}{(1+e_2\overline{\eta_2}+f_2\overline{\eta_3})(1+\beta_1\overline{\eta_1})^2}, \\
a_{22} &= \frac{\alpha_1\overline{\eta_1}((1+e_2\overline{\eta_2})^2+f_2\overline{\eta_3}(1+2e_2\overline{\eta_2}))}{(1+\beta_1\overline{\eta_1})(1+e_2\overline{\eta_2}+f_2\overline{\eta_3})} - \frac{\alpha_2\overline{\eta_3}}{(1+\beta_2\overline{\eta_2})^2} - \delta_1, \\
a_{23} &= -\frac{\alpha_1 f_2(1+e_2\overline{\eta_2})\overline{\eta_1}\,\overline{\eta_2}}{(1+\beta_1\overline{\eta_1})(1+e_2\overline{\eta_2}+f_2\overline{\eta_3})^2} - \frac{\alpha_2\overline{\eta_2}}{1+\beta_2\overline{\eta_2}}, \\
a_{32} &= \frac{\alpha_2\overline{\eta_3}}{(1+\beta_2\overline{\eta_2})^2}, \quad a_{33} = \frac{\alpha_2\overline{\eta_2}}{1+\alpha_2\overline{\eta_2}} - \delta_2.
\end{aligned}$$

Lemma 1. *The species-free equilibrium point* $E_0(0,0,0)$ *is unstable for* $0 < \alpha \le 1$.

Proof. At the point $E_0(0,0,0)$, the characteristic polynomial in view of Equation (14) is $(\lambda+\delta_1)(\lambda+\delta_2)(\lambda_1-1) = 0$. The eigenvalues are $\lambda_1 = -\delta_1$, $\lambda_2 = -\delta_2$, and $\lambda_3 = 1$. According to Theorem 2, $\arg(\lambda_1) = \arg(\lambda_2) = \pi > \frac{\alpha\pi}{2}$ and $\arg(\lambda_3) = 0 < \frac{\alpha\pi}{2}$. Thus, the point E_0 is unstable for $0 < \alpha \le 1$. □

Lemma 2. *The predator-free equilibrium point* $E_1(1,0,0)$ *is unstable for* $0 < \alpha \le 1$ *if* $\delta_1 < \frac{\alpha_1}{\beta_1+1}$.

Proof. The equilibrium point $E_1(1,0,0)$ is free from middle and special predators. The following characteristic equation at the point E_1 is obtained:

$$(\delta_2+\lambda)(\lambda+1)\frac{(\delta_1-\alpha_1+\lambda+\beta_1\delta_1+\beta_1\lambda)}{\beta_1+1} = 0. \tag{15}$$

The eigenvalues of Equation (15) are $\lambda_1 = -\delta_2$, $\lambda_2 = -1$ and $\lambda_3 = -\delta_1 + \frac{\alpha_1}{\beta_1+1}$. If $\delta_1 < \frac{\alpha_1}{\beta_1+1}$, then $\arg(\lambda_3) = 0 < \frac{\alpha\pi}{2}$. Moreover, if $\delta_1 > \frac{\alpha_1}{\beta_1+1}$, then $\arg(\lambda_3) = 0 < \frac{\alpha\pi}{2}$. In view of Theorem 2, the equilibrium point E_1 is unstable for $\delta_1 < \frac{\alpha_1}{\beta_1+1}$. □

Note 1: The characteristic equation of the above two propositions does not include fear-related terms for the equilibrium point. Therefore, the system exhibits identical dynamic behavior in both cases, with or without fear-related terms.

Lemma 3. *The special predator-free equilibrium $E_2 = (\eta_{21}, \eta_{22}, 0)$ is unstable for $0 < \alpha \leq 1$ when the fear terms and the fear-induced COE parameters are $f_1 = 0.5$, $f_2 = 0$, $e_1 = 0$, and $e_2 = 0$.*

Proof. Consider the following fear-related terms $f_1 = 0.5$, $f_2 = 0$, $e_1 = 0$, and $e_2 = 0$. Other parameters are $\alpha_1 = 5$, $\alpha_2 = 0.1$, $\beta_1 = 3$, $\beta_2 = 2$, $\delta_1 = 0.4$, and $\delta_2 = 0.01$. The equilibrium point $E_2(0.1053, 0.2128, 0)$ is acquired, and the characteristic equation at E_2 is $\lambda^3 - 0.1039\lambda^2 + 0.26997\lambda - 0.00133 = 0$. The eigenvalues are $\lambda_1 = 0.0049$, $\lambda_2 = 0.0495 + 0.5168i$, and $\lambda_3 = 0.0495 - 0.5168i$. Because $\arg(\lambda_1) = 0 < \frac{\alpha\pi}{2}$, for every $0 < \alpha \leq 1$. According to Theorem 2, the point is unstable for $0 < \alpha \leq 1$. □

Lemma 4. *The special predator-free equilibrium point $E_2 = (\eta_{21}, \eta_{22}, 0)$ is unstable for $0 < \alpha \leq 1$ when the fear-related parameters are $f_1 = 3.5$, $f_2 = 0$, $e_1 = 1.4$, and $e_2 = 0$.*

Proof. Let us choose the following fear terms and the fear-induced COE parameters $f_1 = 3.5$, $f_2 = 0$, $e_1 = 1.4$, and $e_2 = 0$, while other parameters are selected from Equation (6). Now, the equilibrium point E_2 is $E_2(0.1053, 1.9436, 0)$, and the characteristic equation at E_2 is $\lambda^3 + 5.4553\lambda^2 + 2.1156\lambda - 0.06784 = 0$. The eigenvalues are $\lambda_1 = -5.0332$, $\lambda_2 = -0.4529$, and $\lambda_3 = 0.0298$. As per Theorem 2, the equilibrium point $E_2(0.1053, 1.9436, 0)$ is unstable for $0 < \alpha \leq 1$. □

Lemma 5. *For parameters $\alpha_1 = 5$, $\alpha_2 = 0.1$, $\beta_1 = 3$, $\beta_2 = 2$, $\delta_1 = 0.4$, $\delta_2 = 0.01$, $f_1 = 0$, $f_2 = 0$, $e_1 = 0$, and $e_2 = 0$. The special predator-free equilibrium point $E_2 = (\eta_{21}, \eta_{22}, 0)$ is stable for $0 < \alpha \leq 1$.*

Proof. After taking the arguments in the proposition, the characteristic equation at point $E_2(\frac{4}{38}, 0, 0)$ is $\lambda^3 - 0.7794\lambda^2 - 0.0078\lambda = 0$. Thus, the eigenvalues of the characteristic equation are $\lambda_1 = 0.7895$, $\lambda_2 = 0$, and $\lambda_3 = -0.01$. According to Theorem 2, the equilibrium point $E_2(\frac{4}{38}, 0, 0)$ is unstable for every $0 < \alpha \leq 1$. □

Lemma 6. *The coexistence equilibrium point $E_3 = (\eta_1^*, \eta_2^*, \eta_3^*)$ is stable for $\alpha < 0.9531$ when the fear terms and the fear-induced COE parameters are $f_1 = 3.5$, $f_2 = 0.1$, $e_1 = 1.0$, and $e_2 = 1.4$.*

Proof. The equilibrium point E_3 is $E_3(0.7627, 0.125, 5.0228)$ with $f_1 = 3.5$, $f_2 = 0.1$, $e_1 = 1.0$, and $e_2 = 1.4$. The characteristic equation at E_3 is the following:

$$\lambda^3 + 0.3351\lambda^2 + 0.00263\lambda + 0.0024 = 0. \tag{16}$$

From the above characteristic equation, the respective eigenvalues are $\lambda_1 = -0.3473$, $\lambda_2 = 0.0061 + 0.0827i$ and $\lambda_3 = 0.0061 - 0.0827i$. Thus, $\arg(\lambda_1) = \pi > \frac{\alpha\pi}{2}$ and $|\arg(\lambda_{2,3})| = 1.4972 > \frac{\alpha\pi}{2}$ for $\alpha < 0.9531$. Moreover, from Theorem 2, the point $E_3(0.7627, 0.125, 5.0228)$ is stable for $\alpha < 0.9531$. □

Lemma 7. *The coexistence equilibrium point $E_3 = (\eta_1^*, \eta_2^*, \eta_3^*)$ is stable for $\alpha < 0.9269$ with the fear-related parameters $f_1 = 3.5$, $f_2 = 0$, $e_1 = 2.1$ and $e_2 = 0$.*

Proof. The rest of the parameters are selected from Equation (6) when the fear-related terms are selected in the proposition. The equilibrium point $E_3 = (0.7824, \frac{1}{8}, 9.6090)$, and the characteristic equation at E_3 is given below:

$$\lambda^3 + 0.3701\lambda^2 + 0.0001\lambda + 0.0032 = 0. \tag{17}$$

The eigenvalues of Equation (17) are $\lambda_1 = -0.3910$ and $\lambda_{2,3} = 0.0104 \pm 0.0902i$. Due to $\arg(\lambda_1) = \pi > \frac{\alpha\pi}{2}$ and $|\arg(\lambda_{2,3})| = 1.4560 > \frac{\alpha\pi}{2}$ for $\alpha < 0.9269$. Moreover, from Theorem 2, the point E_3 is stable for $\alpha < 0.9269$. □

Lemma 8. *The coexistence equilibrium point $E_3 = (\eta_1^*, \eta_2^*, \eta_3^*)$ is stable for $\alpha < 0.6960$, with fear terms and the fear-induced COE parameters are $f_1 = 0$, $f_2 = 0$, $e_1 = 0$, and $e_2 = 0$.*

Proof. The equilibrium point $E_3(0.8192, 0.1250, 9.8075)$ is obtained when the rest of the parameters are the same as in Equation (6). The characteristic equation at E_3 is $\lambda^3 + 0.5337\lambda^2 - 0.0402\lambda + 0.0043 = 0$. The eigenvalues are $\lambda_1 = -0.6111$ and $\lambda_{2,3} = 0.0387 \pm 0.0748i$. Moreover, $\arg(\lambda_1) = \pi > \frac{\alpha\pi}{2}$ and $|\arg(\lambda_{2,3})| = 1.0933 > \frac{\alpha\pi}{2}$ for $\alpha < 0.6960$. According to Theorem 2, the equilibrium point $E_3 = (0.8192, \frac{1}{8}, 9.8075)$ is stable for $\alpha < 0.9269$. □

5. Hopf Bifurcation

In this section, let us take e_1 as the bifurcation parameter and fix other parameters. In this way, the condition for a Hopf bifurcation can be established to occur at the equilibrium point E_3. The Jacobian matrix of the system (7) at any point $E_3(\eta_1^*, \eta_2^*, \eta_3^*)$ is given by the following expression:

$$J(\overline{E}) = \begin{bmatrix} a_1 & -a_2 & 0 \\ a_3 & a_4 & -a_5 \\ 0 & a_6 & 0 \end{bmatrix}, \tag{18}$$

where

$$\begin{aligned}
a_1 &= \frac{1 - 2\eta_1 + 2e_1^*\eta_1^* - 3e_1\eta_1^{*2}}{1 + e_1\eta_1^* + f_1\eta_2^*} - \frac{e_1\eta_1^*(1-\eta_1^*)(1+e_1\eta_1^*)}{(1 + e_1\eta_1^* + f_1\eta_2^*)^2} - \frac{\alpha_1\eta_2^*}{(1+\beta_1\eta_1^*)^2}, \\
a_2 &= \frac{f_1\eta_1^*(1-\eta_1^*)(1+e_1\eta_1^*)}{(1 + e_1\eta_1^* + f_1\eta_2^*)^2} + \frac{\alpha_1\eta_1^*}{1+\beta_1\eta_1^*}, \quad a_3 = \frac{\alpha_1(1+e_2\eta_2^*)\eta_2^*}{(1+e_2\eta_2^* + f_2\eta_3^*)(1+\beta_1\eta_1^*)^2}, \\
a_4 &= \frac{\alpha_1 e_2 f_2 \eta_1^*\eta_2^*\eta_3^*}{(1+\beta_1\eta_1^*)(1+e_2\eta_2^* + f_2\eta_3^*)^2} + \frac{\alpha_2\beta_2\eta_2^*\eta_3^*}{(1+\beta_2\eta_2^*)^2}, \\
a_5 &= \frac{\alpha_1 f_2(1+e_2\eta_2^*)\eta_1^*\eta_2^*}{(1+\beta_1\eta_1^*)(1+e_2\eta_2^* + f_2\eta_3^*)^2} + \frac{\alpha_2\eta_2^*}{1+\beta_2\eta_2^*}, \quad a_6 = \frac{\alpha_2\eta_3^*}{(1+\beta_2\eta_2^*)^2}.
\end{aligned}$$

The characteristic polynomial for Equation (18) at the equilibrium point E_3 is given below:

$$\lambda^3 + R_1\lambda^2 + R_2\lambda + R_3 = 0. \tag{19}$$

The discriminant $D(P)$ can be defined using the fractional-order Routh–Hurwitz conditions [40]:

$$D(P) = 18R_1R_2R_3 + (R_1R_2)^2 - 4R_3R_1^3 - 4R_2^3 - 27R_3^2, \tag{20}$$

where

$$R_1 = -(a_1 + a4),\ R_2 = a_1a_4 + a_2a_3 + a_5a_6,\ R_3 = -a_1a_5a_6.$$

Theorem 3. *When a bifurcation parameter e_1 passes through the critical value e_1^*, the fractional-order system (7) undergoes a Hopf bifurcation at the equilibrium point $E_3(\eta_1^*, \eta_2^*, \eta_3^*)$, if the following conditions hold:*

(a) *The corresponding characteristic Equation (19) has a pair of complex conjugate roots $\lambda_{1,2} = \theta \pm \omega i$, where $\theta > 0$, and one negative real root λ_3;*

(b) $u(\alpha, e_1) = \frac{\pi}{2}\alpha - \min\limits_{1\le i\le 3}|\arg(\lambda_i)| = 0$;

(c) $\frac{\mathrm{d}u(e_1)}{\mathrm{d}e_1}\big|_{e_1=e_1^*} \neq 0$ *(transversality condition).*

Proof. If Equation (19) has a pair of complex conjugate roots $\lambda_{1,2} = \theta \pm i\omega$ with $\theta > 0$ and a negative root λ_3. Using the previously reported results [40], if $D(P) < 0$, the Equation (19) has a pair of complex conjugate roots $\lambda_{1,2}$ and one real root λ_3. From the relationship between the roots and the coefficients, it is known that $\lambda_1\lambda_2\lambda_3 = -R_3 = a_1a_5a_6$. Hence, $\lambda_3 < 0$ if $a_1a_5a_6 < 0$.

Now, we want to make sure the condition (b) is satisfied. The critical value e_1^* can be described in the following fashion:

$$u(e_1^*) = \alpha\frac{\pi}{2} - \min_{1\leq i\leq 3}|\arg(\lambda_i(e_1^*))| = \alpha\frac{\pi}{2} - \arctan|\frac{\omega(e_1^*)}{\theta(e_1^*)}| = 0 \tag{21}$$

and

$$\tan^2(\frac{\alpha\pi}{2}) = \frac{\omega^2(e_1^*)}{\theta^2(e_1^*)}. \tag{22}$$

For Equation (19), the following relations can be obtained from the relationship between roots and coefficients:

$$\begin{cases} \theta^2 + \omega^2 + 2\theta\lambda_3 = R_2, \\ (\theta^2 + \omega^2)\lambda_3 = -R_3, \\ 2\theta + \lambda_3 = -R_1. \end{cases} \tag{23}$$

Combined with Equation (22), the following expressions can be computed:

$$\theta(e_1) = \frac{-2R_3}{(R_2 - \tan^2\frac{\alpha\pi}{2})(1 + \tan^2\frac{\alpha\pi}{2})}, \tag{24}$$

$$\omega^2(e_1) = R_2 - \frac{12R_3^2}{(R_2 - \tan^2\frac{\alpha\pi}{2})^2(1 + \tan^2\frac{\alpha\pi}{2})^2} + \frac{-4R_1R_3}{(R_2 - \tan^2\frac{\alpha\pi}{2})(1 + \tan^2\frac{\alpha\pi}{2})}, \tag{25}$$

where e_1 is a bifurcation parameter. The critical value e_1^* can be solved from the following relation $\frac{\omega^2(e_1^*)}{\theta^2(e_1^*)} = \frac{\alpha\pi}{2}$. The condition (c) guarantees that the sign of $u(e_1)$ can change when the bifurcation parameter e_1 passes through the critical value e_1^*. In summary, we can be reiterated that a Hopf bifurcation of system (7) occurs at $e_1 = e_1^*$.

In the second scenario, when the fractional-order parameter α passes through $\alpha^* = \frac{2}{\pi}\arctan|\frac{\omega}{\theta}|$, the fractional-order system (7) undergoes a Hopf bifurcation. The distinction between fractional and integer-order systems lies in the behavior of their limit cycles, while the limit cycle of an integer-order system can serve as a solution to the system, in a fractional-order system, the trajectory only approaches the limit cycle without becoming the exact solution of the fractional-order system. Moreover, the fractional system at $0 < \alpha < \alpha^*$ is stable. In other words, it is possible to produce limit cycles only for $\alpha \geq \alpha^*$. □

6. Chaos Control

Consider the following controlled system with control functions $u_1(t)$, $u_2(t)$, $u_3(t)$:

$$\begin{aligned} \frac{d^\alpha\eta_1}{dt^\alpha} &= \eta_1\left((1-\eta_1)\cdot\frac{1+e_1\eta_1}{1+e_1\eta_1+f_1\eta_2} - \frac{\alpha_1\eta_2}{1+\beta_1\eta_1}\right) + u_1(t), \\ \frac{d^\alpha\eta_2}{dt^\alpha} &= \eta_2\left(\frac{\alpha_1\eta_1}{1+\beta_1\eta_1}\cdot\frac{1+e_2\eta_2}{1+e_2\eta_2+f_2\eta_3} - \delta_1 - \frac{\alpha_2\eta_3}{1+\beta_2\eta_2}\right) + u_2(t), \\ \frac{d^\alpha\eta_3}{dt^\alpha} &= \eta_3\left(\frac{\alpha_2\eta_2}{1+\beta_2\eta_2} - \delta_2\right) + u_3(t), \end{aligned} \tag{26}$$

where $(\overline{\eta_1}, \overline{\eta_2}, \overline{\eta_3})$ is the solution of system (7).

Now, the error functions are defined as $e_1 = \eta_1 - \overline{\eta_1}$, $e_2 = \eta_2 - \overline{\eta_2}$, and $e_3 = \eta_3 - \overline{\eta_3}$. The following error systems can be defined:

$$\begin{cases} \dfrac{\mathrm{d}^\alpha e_1}{\mathrm{d}t^\alpha} = \eta_1\left((1-\eta_1)\cdot\dfrac{1+e_1\eta_1}{1+e_1\eta_1+f_1\eta_2} - \dfrac{\alpha_1\eta_2}{1+\beta_1\eta_1}\right) + u_1(t) \\ \qquad - \overline{\eta_1}\left((1-\overline{\eta_1})\cdot\dfrac{1+e_1\overline{\eta_1}}{1+e_1\overline{\eta_1}+f_1\overline{\eta_2}} - \dfrac{\alpha_1\overline{\eta_2}}{1+\beta_1\overline{\eta_1}}\right), \\ \dfrac{\mathrm{d}^\alpha e_2}{\mathrm{d}t^\alpha} = \eta_2\left(\dfrac{\alpha_1\eta_1}{1+\beta_1\eta_1}\cdot\dfrac{1+e_2\eta_2}{1+e_2\eta_2+f_2\eta_3} - \delta_1 - \dfrac{\alpha_2\eta_3}{1+\beta_2\eta_2}\right) + u_2(t) \\ \qquad - \overline{\eta_2}\left(\dfrac{\alpha_1\overline{\eta_1}}{1+\beta_1\overline{\eta_1}}\cdot\dfrac{1+e_2\overline{\eta_2}}{1+e_2\overline{\eta_2}+f_2\overline{\eta_3}} - \delta_1 - \dfrac{\alpha_2\overline{\eta_3}}{1+\beta_2\overline{\eta_2}}\right), \\ \dfrac{\mathrm{d}^\alpha e_3}{\mathrm{d}t^\alpha} = \eta_3\left(\dfrac{\alpha_2\eta_2}{1+\beta_2\eta_2} - \delta_2\right) + u_3(t) - \overline{\eta_3}\left(\dfrac{\alpha_2\overline{\eta_2}}{1+\beta_2\overline{\eta_2}} - \delta_2\right). \end{cases} \tag{27}$$

Theorem 4. *The error system (27) converges to zero if the control functions are considered as follows:*

$$\begin{cases} u_1(t) = -e_1 - \eta_1\left((1-\eta_1)\cdot\dfrac{1+e_1\eta_1}{1+e_1\eta_1+f_1\eta_2} - \dfrac{\alpha_1\eta_2}{1+\beta_1\eta_1}\right) \\ \qquad + \overline{\eta_1}\left((1-\overline{\eta_1})\cdot\dfrac{1+e_1\overline{\eta_1}}{1+e_1\overline{\eta_1}+f_1\overline{\eta_2}} - \dfrac{\alpha_1\overline{\eta_2}}{1+\beta_1\overline{\eta_1}}\right), \\ u_2(t) = -\eta_2\left(\dfrac{\alpha_1\eta_1}{1+\beta_1\eta_1}\cdot\dfrac{1+e_2\eta_2}{1+e_2\eta_2+f_2\eta_3} - \dfrac{\alpha_2\eta_3}{1+\beta_2\eta_2}\right) \\ \qquad + \overline{\eta_2}\left(\dfrac{\alpha_1\overline{\eta_1}}{1+\beta_1\overline{\eta_1}}\cdot\dfrac{1+e_2\overline{\eta_2}}{1+e_2\overline{\eta_2}+f_2\overline{\eta_3}} - \dfrac{\alpha_2\overline{\eta_3}}{1+\beta_2\overline{\eta_2}}\right), \\ u_3(t) = -\eta_3\left(\dfrac{\alpha_2\eta_2}{1+\beta_2\eta_2}\right) + \overline{\eta_3}\left(\dfrac{\alpha_2\overline{\eta_2}}{1+\beta_2\overline{\eta_2}}\right). \end{cases} \tag{28}$$

Proof. The following Lyapunov function can be defined as:

$$V = \frac{1}{2}\left(e_1^2 + e_2^2 + e_3^2\right). \tag{29}$$

Taking the fractional derivative with respect to V as per the fractional derivative definition, yield the following expression:

$$\frac{\mathrm{d}^\alpha V}{\mathrm{d}t^\alpha} \le e_1\frac{\mathrm{d}^\alpha e_1}{\mathrm{d}t^\alpha} + e_2\frac{\mathrm{d}^\alpha e_2}{\mathrm{d}t^\alpha} + e_3\frac{\mathrm{d}^\alpha e_3}{\mathrm{d}t^\alpha}. \tag{30}$$

The following equation results in after substituting Equation (27) into the above equation:

$$\frac{\mathrm{d}^\alpha V}{\mathrm{d}t^\alpha} \le -e_1^2 - \delta_1 e_2^2 - \delta_2 e_3^2 < 0. \tag{31}$$

Therefore, the trajectories (η_1, η_2, η_3) converges to a point $(\eta_1^*, \eta_2^*, \eta_3^*)$. Moreover, the periodic orbital that was unstable at the equilibrium point can be stabilized by controlling this convergence. □

7. Numerical Simulation

In this section, MATLAB is employed for numerical simulations to investigate diverse, complex dynamic behaviors of the system under study by manipulating system parameters. Incorporating fractional-order in the system enables a more authentic representation of predator–prey dynamics. It should be noted that for the convenience of handling the system (4), we have transformed some variables. When working with real data, refer to the relationships between the variables described in this article.

According to the fractional-order stability theory, parameters $f_1 = 3.5$, $f_2 = 0.1$, $e_1 = 1$, and $e_2 = 1.4$ should be used, while other parameters are the same as in Equation (6). The necessary condition for the system (7) to reach an unstable state is $\alpha \geq 0.9531$. Therefore, the order $\alpha = 0.9531$ is the minimum order for the system to reach unstable state. Figure 3a gives the system phase diagram of $\alpha = 0.9$ and verifies the stability condition of Lemma 6. As a comparison, the order $\alpha = 0.99$ is selected, and the periodic oscillation for $\alpha = 0.99$ can be seen in Figure 4a. Similarly, let us verify Lemma 7. The minimum order for system (7) to reach the unstable state is $\alpha = 0.9269$. Therefore, the order $\alpha = 0.9$ was selected, as shown in Figure 3b. For comparison, the system phase diagram with the order $\alpha = 0.99$ is drawn, as shown in Figure 4b. The observation shows that the result accords with the conclusion of Lemma 7. In the same way, it is pretty straightforward to verify Lemma 8 by taking the order $\alpha = 0.65$ in Figure 3c and $\alpha = 0.99$ in Figure 4c.

Figure 5 shows that the numerical solutions are converging to $E_1 = (1, 0, 0)$. We present numerical simulations of fractional-order system (7) using time series plots for all state variables to illustrate some of the results obtained. Except for $\delta_1 = 1.5$, the rest of the parameters are the same as those taken in Figure 4b. α changes from $\alpha = 0.75$ to $\alpha = 1$, as shown in Figure 5. With the increase of fractional-order α, the convergence rate of the state solution to the equilibrium point is faster. We conclude that the derivative order α can play a role in understanding the history and dynamics of populations.

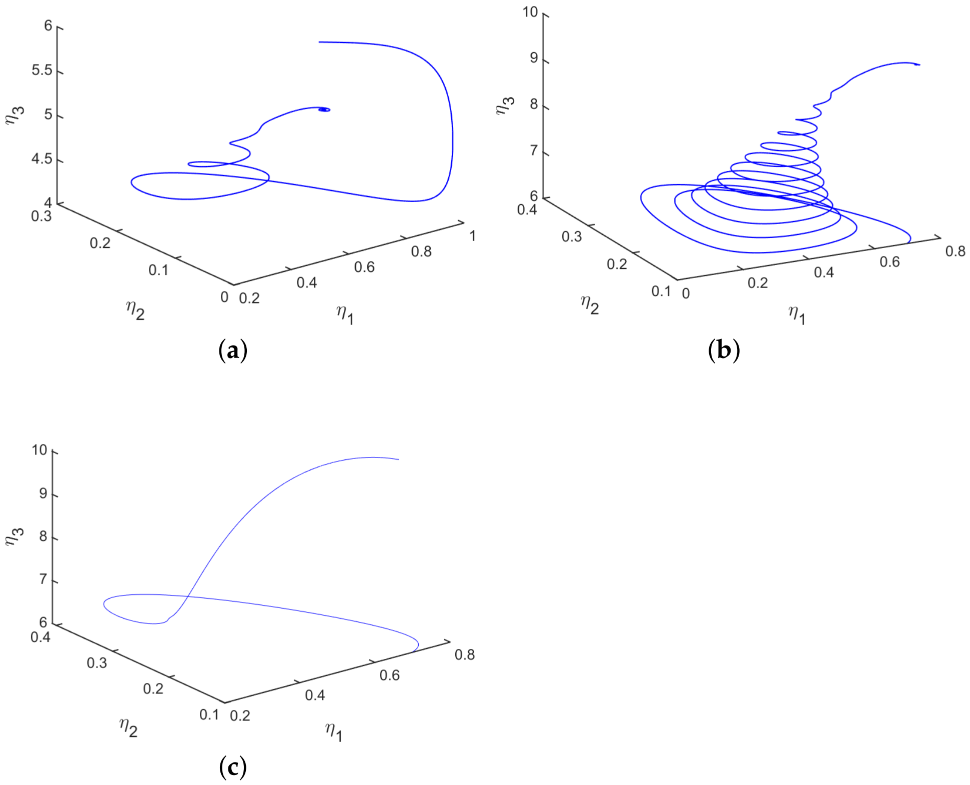

Figure 3. The chaotic attractor phase diagrams of the system (7): (**a**) LAS for $\alpha = 0.9$, $f_1 = 3.5$, $f_2 = 0.1$, $e_1 = 1.0$, and $e_2 = 1.4$, (**b**) LAS for $\alpha = 0.9$, $f_1 = 3.5$, $f_2 = 0$, $e_1 = 2.1$, and $e_2 = 0$, and (**c**) LAS for $\alpha = 0.65$, $f_1 = 0$, $f_2 = 0$, $e_1 = 0$, and $e_2 = 0$.

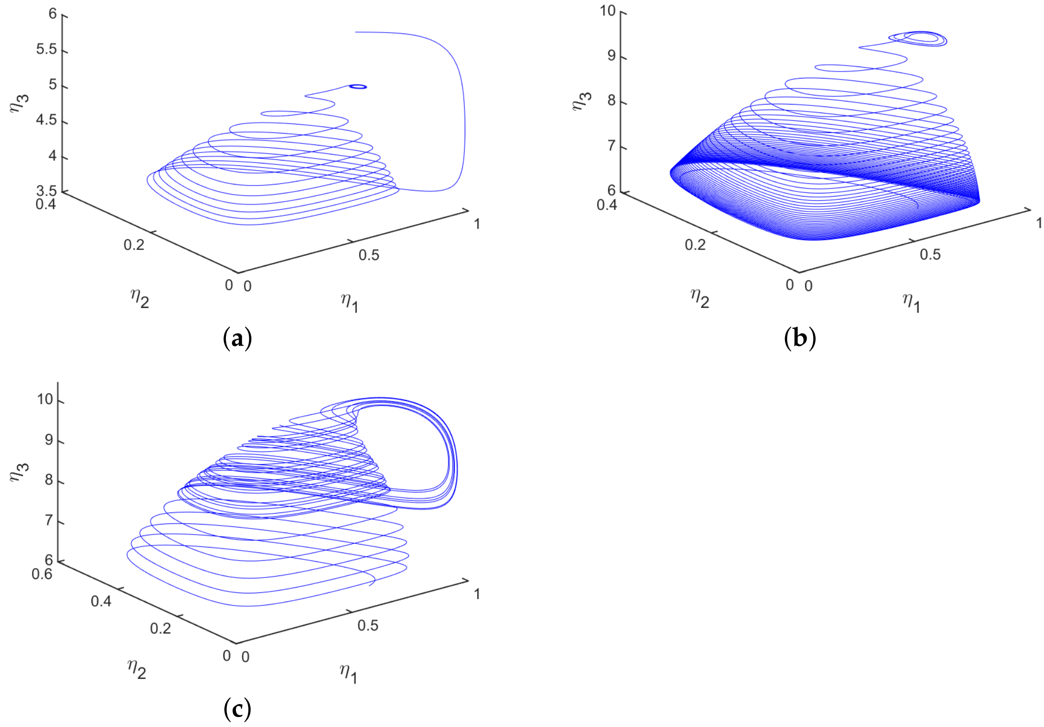

Figure 4. The chaotic attractor phase diagrams of the system (7) at $\alpha = 0.99$: (**a**) $f_1 = 3.5$, $f_2 = 0.1$, $e_1 = 1.0$, and $e_2 = 1.4$, (**b**) $f_1 = 3.5$, $f_2 = 0$, $e_1 = 2.1$, and $e_2 = 0$, and (**c**) $f_1 = 0$, $f_2 = 0$, $e_1 = 0$, and $e_2 = 0$.

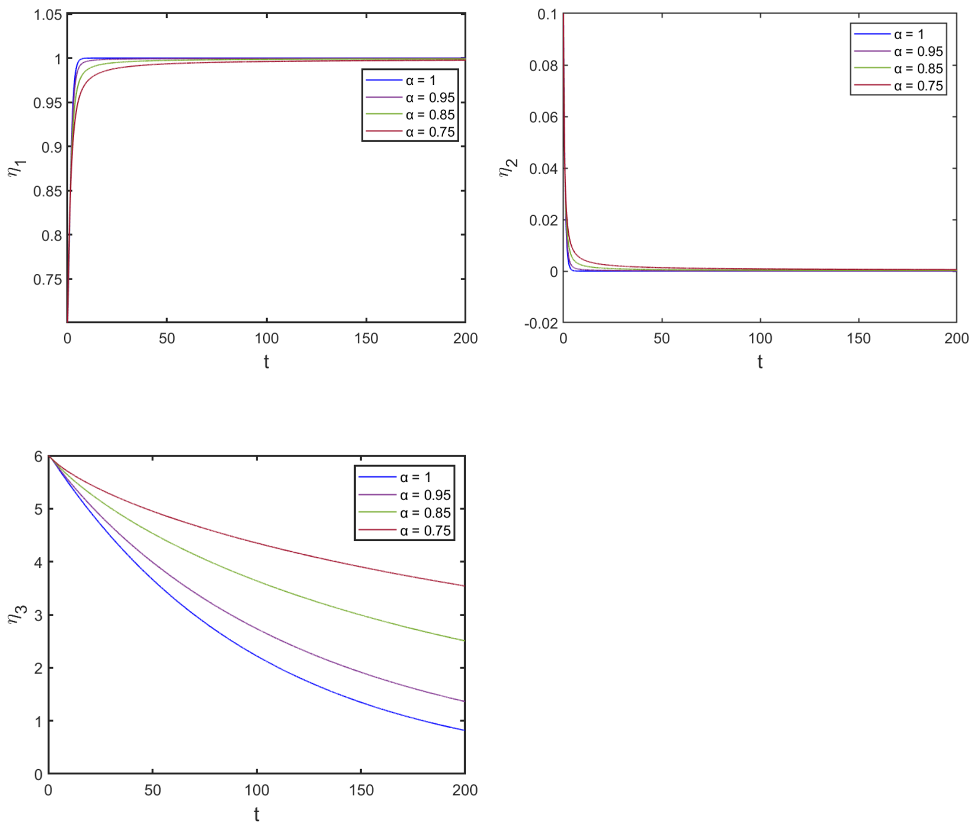

Figure 5. Adam–Bashforth–Moulton numerical results of system (7) via a Caputo fractional operator for different fractional-order α values.

The dynamic behavior of the system (7) when the order is $\alpha = 0.99$ is shown in Figure 4. After applying the chaotic control, it can be seen from Figure 6 that the unstable trajectory is controlled at the equilibrium point. If the fear-induced COE parameters $e_1 = 0$ and $e_2 = 0$ are considered, then the system (7) is reduced to a fractional-order three-species food chain model with fear, which has been discussed by Mishra et al. [27].

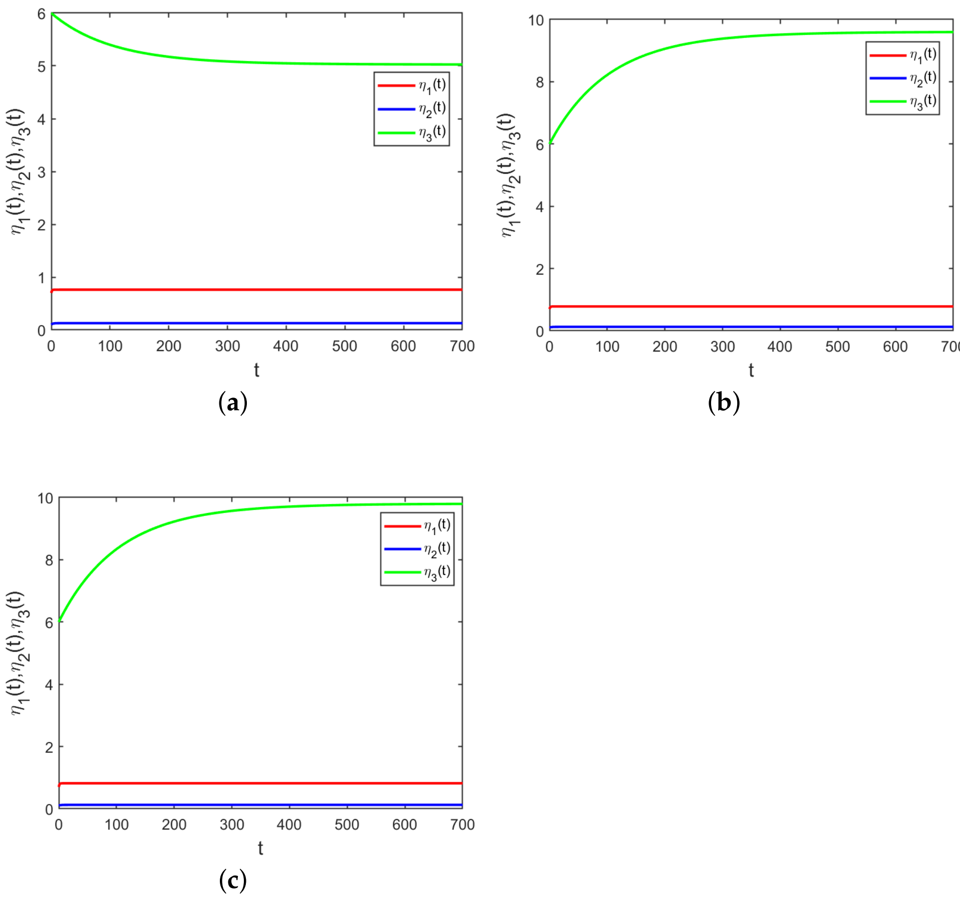

Figure 6. The plot of the control trajectories η_1, η_2, and η_3 of the system (7): (**a**) at the equilibrium point $E_3 = (0.7627, 0.125, 5.0228)$, (**b**) at the equilibrium point $E_3 = (0.7824, 0.125, 9.6090)$, and (**c**) at the equilibrium point $E_3 = (0.8192, 0.125, 9.8075)$.

8. Conclusions

This work examines the fractional three-population food chain model with fear and its carry-over effects, analyzing the stability of system under different fear terms and its carry-over effect (COE) parameters. The findings emphasize the significance of the order in determining system dynamics parameters. Predator fear and COE influences the growth rates of prey and intermediate predators, resulting in the emergence of complex dynamic behaviors. Furthermore, this study provides analytical conditions for a Hopf bifurcation in fractional-order systems, revealing chaotic behavior across various orders. Additionally, by incorporating mixed control elements into the fractional-order system from an equilibrium standpoint, this study demonstrates the stability of the fractional-order system with chaos control through numerical simulations and illustrations.

Author Contributions: Conceptualization, Z.C. and Y.Z.; methodology, Z.C.; software, Z.C. and R.L.; formal analysis, R.L. and Y.Z.; investigation, Z.C.; data curation, Z.C.; writing original draft preparation, Z.C.; writing review and editing, R.L. and Y.Z.; supervision, Y.Z.; funding acquisition, Z.C. and Y.Z. All authors have read and agreed to the published version of the manuscript.

Funding: The authors gratefully acknowledge the support of the National Natural Science Foundation of China through grant No. 11962025, the Key project of Natural Science Foundation of Inner

Mongolia Autonomous Region through grant No. 2022ZD05, and the Fundamental Research Funds for the Inner Mongolia Normal University through grant No. 2023JBBJ004.

Data Availability Statement: Not applicable.

Conflicts of Interest: The authors declare that there are no conflict of interest regarding the publication of this paper.

References

1. Ramasamy, S.; Banjerdpongchai, D.; Park, P.G. Chaos Control of a Delayed Tri-Trophic Food Chain Model with Fear and Its Carry Over Effects. *Symmetry* **2023**, *15*, 484. [CrossRef]
2. Ali, N.; Chakravarty, S. Stability analysis of a food chain model consisting of two competitive preys and one predator. *Nonlinear Dyn.* **2015**, *82*, 1303–1316. [CrossRef]
3. Holmes, E.E.; Lewis, M.A.; Banks, J.E.; Veit, D. Partial differential equations in ecology: Spatial interactions and population dynamics. *Ecology* **1994**, *75*, 17–29. [CrossRef]
4. Jassim, H.K.; Abdulshareef Hussein, M. A New Approach for Solving Nonlinear Fractional Ordinary Differential Equations. *Mathematics* **2023**, *11*, 1565. [CrossRef]
5. Johansyah, M.D.; Sambas, A.; Mobayen, S.; Vaseghi, B.; Al-Azzawi, S.F.; Sukono; Sulaiman, I.M. Dynamical Analysis and Adaptive Finite-Time Sliding Mode Control Approach of the Financial Fractional-Order Chaotic System. *Mathematics* **2023**, *11*, 100. [CrossRef]
6. Song, H.; Hu, C.; Yu, J. Stability and Synchronization of Fractional-Order Complex-Valued Inertial Neural Networks: A Direct Approach. *Mathematics* **2022**, *10*, 4823. [CrossRef]
7. Borah, M.; Gayan, A.; Sharma, J.S.; Chen, Y.; Wei, Z.; Pham, V.-T. Is fractional-order chaos theory the new tool to model chaotic pandemics as COVID-19? *Nonlinear Dyn.* **2022**, *109*, 1187–1215. [CrossRef]
8. Li, L.; Chen, Y.; Zhou, B.; Liu, H.; Liu, Y. Linearization threshold condition and stability analysis of a stochastic dynamic model of one-machine infinite-bus (OMIB) power systems. *Protec. Control Mod. Power Syst.* **2021**, *6*, 1–11. [CrossRef]
9. Yi, T.; Zuwang, W. Effect of time delay and evolutionarily stable strategy. *J. Theor. Biol.* **1997**, *187*, 111–116. [CrossRef]
10. Song, G.; Tao, G. A partial-state feedback model reference adaptive control scheme. *IEEE Trans. Automat. Contr.* **2019**, *65*, 44–57. [CrossRef]
11. Li, Y.; Wei, Z.; Aly, A.A. A 4D hyperchaotic Lorenz-type system: Zero-Hopf bifurcation, ultimate bound estimation, and its variable-order fractional network. *Eur. Phys. J. Spec. Top.* **2022**, *231*, 1847–1858. [CrossRef]
12. Holling, C.S. The components of predation as revealed by a study of small-mammal predation of the European Pine Sawfly. *Can. Entomol.* **1959**, *91*, 293–320. [CrossRef]
13. Hastings, A.; Powell, T. Chaos in a three-species food chain. *Ecology* **1991**, 72, 896–903. [CrossRef]
14. Xiu, C.; Zhou, R.; Liu, Y. New chaotic memristive cellular neural network and its application in secure communication system. *Chaos Solitons Fractals* **2020**, *141*, 110316. [CrossRef]
15. Piccardi, C.; Lazzaris, S. Vaccination policies for chaos reduction in childhood epidemics. *IEEE. Trans. Biomed. Eng.* **1998**, *45*, 591–595. [CrossRef] [PubMed]
16. Ghosh, K.; Biswas, S.; Samanta, S.; Tiwari, P.K.; Alshomrani, A.S.; Chattopadhyay, J. Effect of multiple delays in an eco-epidemiological model with strong Allee effect. *Int. J. Bifurcat. Chaos* **2017**, *27*, 1750167. [CrossRef]
17. Suraci, J.P.; Clinchy, M.; Dill, L.M.; Roberts, D.; Zanette, L.Y. Fear of large carnivores causes a trophic cascade. *Nat. Common.* **2016**, *7*, 10698. [CrossRef]
18. Wang, X.; Zanette, L.; Zou, X. Modelling the fear effect in predator-prey interactions. *J. Math. Biol.* **2016**, *73*, 1179–1204. [CrossRef]
19. Panday, P.; Pal, N.; Samanta, S.; Chattopadhyay, J. A three species food chain model with fear induced trophic cascade. *Int. J. Appl. Comput. Math.* **2019**, *5*, 1–26. [CrossRef]
20. Sasmal, S.K.; Takeuchi, Y. Modeling the Allee effects induced by cost of predation fear and its carry-over effects. *J. Math. Anal. Appl.* **2022**, *505*, 125485. [CrossRef]
21. Elliott, K.H.; Betini, G.S.; Dworkin, I.; Norris, R. Experimental evidence for within-and cross-seasonal effects of fear on survival and reproduction. *J. Anim. Ecol.* **2016**, *85*, 507–515. [CrossRef] [PubMed]
22. Dubey, B.; Sasmal, S.K. Chaotic dynamics of a plankton-fish system with fear and its carry over effects in the presence of a discrete delay. *Chaos Solitons Fractals* **2022**, *160*, 112245.
23. Mondal, S.; Samanta, G. A comparison study of predator-prey system in deterministic and stochastic environments influenced by fear and its carry-over effects. *Eur. Phys. J. Plus* **2022**, *137*, 70. [CrossRef]
24. Yuan, T.; Yang, H.; Ivanov, I.G. Reachability and Observability of Positive Linear Electrical Circuits Systems Described by Generalized Fractional Derivatives. *Mathematics* **2021**, *9*, 2856. [CrossRef]
25. [CrossRef] Wang, B.; Sajjadi, S.S.; Jahanshahi, H.; Karaca, Y.; Hou, D.; Pi, L.; Xia, W.F.; Aly, A.A.; Taylor, T. Predictive Control of The Variable-Order Fractional Chaotic Ecological System. *Fractals* **2022**, *30*, 2240178.
26. Alidousti, J.; Mostafavi Ghahfarokhi, M. Dynamical behavior of a fractional three-species food chain model. *Nonlinear Dyn.* **2019**, *95*, 1841–1858. [CrossRef]

27. Mishra, A.K.; Kumar, R.; Yadav, V.K. Stability Analysis and Controlling Chaos of Fractional-Order Three-Species Food Chain Model with Fear. *Int. J. Appl. Comput. Math* **2021**, *7*, 214. [CrossRef]
28. Papoulia, K.D.; Panoskaltsis, V.P.; Kurup, N.V.; Korovajchuk, I. Rheological representation of fractional order viscoelastic material models. *Rheol. Acta* **2010**, *49*, 381–400. [CrossRef]
29. Sun, G.; Zhu, Z.H. Fractional order dynamics and control of rigid flexible coupling space structures. *J. Guid. Control Dyn.* **2015**, *38*, 1324–1330. [CrossRef]
30. Almatroud, O.A.; Hioual, A.; Ouannas, A.; Grassi, G. On Fractional-Order Discrete-Time Reaction Diffusion Systems. *Mathematics* **2023**, *11*, 2447. [CrossRef]
31. Hegazi, A.S.; Ahmed, E.; Matouk, A.E. On chaos control and synchronization of the commensurate fractional order Liu system. *Commun. Nonlinear Sci. Numer. Simul.* **2013**, *18*, 1193–1202. [CrossRef]
32. Xu, J.; Ji, G.; Ge, Q. Dynamic behaviors of a fractional order two-species cooperative systems with harvesting. *Chaos Solitons Fractals* **2016**, *92*, 51–55. [CrossRef]
33. Das, S. *Functional Fractional Calculus*; Springer: Berlin/Heidelberg, Germany, 2011.
34. Tavazoei, M.S.; Haeri, M.; Attari, M.; Bolouki, S.; Siami, M. More details on analysis of fractional-order Van der Pol oscillator. *J. Vib. Control* **2009**, *15*, 803–819.
35. Tavazoei, M.S.; Haeri, M. A proof for non existence of periodic solutions in time invariant fractional order systems. *Automatica* **2009**, *45*, 1886–1890. [CrossRef]
36. Tavazoei, M.S. A note on fractional-order derivatives of periodic functions. *Automatica* **2010**, *46*, 945–948. [CrossRef]
37. Aguila-Camacho, N.; Duarte-Mermoud, M.A.; Gallegos, J.A. Lyapunov functions for fractional order systems. *Commun. Nonlin. Sci. Numer. Simul.* **2014**, *19*, 2951–2957. [CrossRef]
38. Matignon, D. Stability results for fractional differential equations with applications to control processing. *Comp. Eng. Syst. Appl.* **1996**, *2*, 963–968. [CrossRef]
39. Naik, P.A.; Zu, J.; Owolabi, K.M. Global dynamics of a fractional order model for the transmission of HIV epidemic with optimal control. *Chaos Solitons Fractals* **2020**, *138*, 109826. [CrossRef]
40. Ahmed, E.; El-Sayed, A.M.A.; El-Saka, H.A.A. On some Routh-Hurwitz conditions for fractional order differential equations and their applications in Lorenz, Rossler, Chua and Chen systems. *Phys. Lett. A* **2006**, *358*, 1–4.